



Unsteady flow of immiscible generalized second-grade fluids in a rectangular channel using fractional derivatives

Imran Siddique^{1,2,3,*}, Laiba Ghafoor¹, Barno Abdullaeva⁴, Aneza Faheem², and Zaher Mundher Yaseen⁵

¹Department of Mathematics, University of Sargodha, Sargodha 40100, Pakistan.

²Department of Mathematics, University of Management and Technology, Lahore 54770, Pakistan.

³Mathematics in Applied Sciences and Engineering Research Group, Scientific Research Center, Al-Ayen University, Nasiriyah, 64001, Iraq.

⁴Department of Mathematics and Information Technologies, Tashkent State Pedagogical University, Tashkent, Uzbekistan.

⁵Civil and Environmental Engineering Department, King Fahd University of Petroleum and Minerals, Dhahran 31261, Saudi Arabia.

Abstract

In this paper, unsteady one-dimensional flows in a rectangular channel of two incompressible and immiscible generalized *second* grade fluids are studied. The generalization discussed consists onto mathematical framework constructed upon constitutive equations of *second*-grade (SG) fluid with temporal fractional derivatives Caputo (C), Caputo-Fabrizio (CF) and Atangna-Baleanu (ABC). The evolution of a shear stress has an impact on the velocity gradient. The velocity and shear stress components are transformed using a Laplace transformation. The Stehfest's numerical approach for the reverse Laplace transformation is used to obtain numerical results for actual velocity and shear stress. The impact of fractional parameters upon velocity and shear stress is investigated using numerical simulations and graphical depictions. The memory impacts are just noticeable for tiny amounts of time t , according to this theory.

Keywords. Fractional calculus, Second-grade fluids, Memory impacts, The flow of two layers.

2010 Mathematics Subject Classification. 65L05, 34K06, 34K28.

1. INTRODUCTION

Fractional calculus as a generalization of the traditional calculus that deals with the non-integer derivative and integral operations. The concept of fractional operators was presented by Lazarevic *et al.* [21]. Fractional calculus is an extension of regular calculus that dates back over 300 years. L'Hospital and Leibniz developed fractional calculus at the consequence on an lengthy discussion in 1695. Elastic moduli and flow-ability, electrodynamics, nutrition, biomechanics and bioinformatics, electro chemical digital signal processing, physics, microelectronics, thermodynamics, and control theory are just a few of the fields where fractional calculus has had a significant impact [6, 13]. In the year 2020, Zafar *et al.* [3] examined the rotary flows for the fractional Maxwell fluid. They used Mathcad software to pictorially interpret the impact of non-integer parameters on velocity and shear stress characteristics.

In manufacturing and engineering applications, non-Newtonian fluids are thought being higher acceptable models of fluids than Newtonian fluids. Such fluids exhibit a non-linear stress - strain relationship pace at any point in the flow. SG fluids are a type of non-Newtonian fluids with the velocity profile has up to 2 derivatives in a stress-strain connection, whereas Newtonian fluids only have first-order derivatives. In many boundary layer flows, the movement of SG fluid attracts the researchers attention, and it has been effectively examined in a variety of flows. In 2016, Abro [2] reported accurate solutions for incompressible SG fluids with porosity due to infinite plate sine and cosine oscillations. Integral transform techniques are utilized to examine and provide precise results for the velocity profile and accompanying shear stress. In 2014, Siddiqui *et al.* [28] studied the two dimensional continuous

Received: 30 June 2025; Accepted: 14 April 2026.

* Corresponding author. Email: imransmsrazi@gmail.com.

flow of an incompressible SG fluid inside a proportionately diverging conduit of changing thickness. In 2020, Bilal *et al.* [8] showed the mass and heat transition characteristics of SG flowing fluid formed from an angled cylinder when diffusion and Joule warming influences were used. They used graphical visualizations to assess the influence from flow-controlling factors on velocity, temperature, and intensity gradients. The shear stress and velocity profile associated with a generalized SG fluid longitudinal oscillatory flow were characterized by Mahmood *et al.* [24]. They plotted velocity profiles to study the influence of various factors upon this flow of regular SG and generalized SG fluids. The organic convective flow of SG fluid inside an vibrating limitless vertical channel were examined by Javaid *et al.* [16]. They graphitized the impact of dimensionless numbers at various time intervals and discovered that velocity of *Newtonian* fluid was greater than velocity for *second* grade fluid. Erdogan and Imrak [11] found a precise solution for flow across dual coaxial cylinders having porosity sides using an incompressible second-grade fluid. The Laplace transformation technique was utilized by Chen *et al.* [10] to solve second-grade flows via a microtube having side slipping. Using the generalized second-grade model and fractional calculus, Nadeem *et al.* [18] investigated the six forms of unstable flows. Khan and Rahman [17] investigated the flow and heat transition of a modified SG fluid in two dimensions across a non-linear stretched sheets having a steady surface temperature.

Matter occurs in a variety of states, referred to as phases, which include gaseous state, liquid state, and solid state. Multiphase fluxes, or simultaneous flows of distinct phases, are common in many practical applications. With the deformation of the interface, two-layer flows cause new instabilities and bifurcations. In a rectangular channel, Luo *et al.* [23] investigated flows unstable one-dimensional flows of dual incompressible and insoluble extended S.G fluid. Luo *et al.* [22] used analytical and numerical approaches to investigate the flow of coupled viscous fluid layers in a two-dimensional channel constrained within a flat and curvy wall. Using numerical techniques, Faryad *et al.* [12] studied the behavior of liquid layers as they encounter a convex corner, accounting for the impact of surface tension. The efficient results for highly formed 2-layer hydraulically flows of inviscid Phan-Thien-Tanner (PTT) fluids in a longitudinal cylindrical conduit were provided by Siddiqui *et al.* [29, 30]. They explained how 2-layers of PTT fluids circulate via a cylindrical conduit to transmit heat.

Fractional operators were widely applied to mathematical modeling of a variety of real-world issues. A variety of complex systems using memory can be explored with time-fractional derivative operators. Fractional calculus became important in microbiology, biochemistry, physics and a range of engineering domains as a result. The concept of fractional operators, as well as their characteristics and applications, is well-presented by Hristov [15], Kilbas *et al.* [19], Povstenko [26, 27], Zheng *et al.* [33], Baleanu *et al.* [5, 7], Hilfer [14], Zafar *et al.* [32], Zhou *et al.* [34] and Nadeem *et al.* [25].

The aim of the paper is to investigate the unsteady 1-dimensional flow in a rectangular channel with immiscible generalized *second* grade fluids. While acting in a flow direction, the channel boundaries undergo variable translating movements in the surfaces. A mathematical framework centered on governing equations having C , CF , and ABC fractional derivatives is used to investigate a extended second-grade fluid flow in which the evolution of a shear stress impacts the velocity field. The velocity and shear stress components were calculated with in Laplace transform domain. The Stehfest's numerical approach for the reverse Laplace transformation is used to obtain numerical results for actual velocity and shear stress.

Numerical simulations and graphical visualizations are utilized to investigate the impacts of fractional factors on velocity and shear stress using the software Mathcad. In comparison to the classical model, the memory effect is substantial in the fractional derivative. Memory effects are shown to be important just over tiny amounts of time t .

2. DESCRIPTION OF METHODOLOGIES

We investigate the one-dimensional continuous flow of extended second grade fluid in the region

$$D_0 = \{(x, y, z) / x \in \mathbf{R}, 0 \leq y \leq d, z \in \mathbf{R}\}.$$

Two adjacent plates in plane $y = 0$ and $y = d$ form the boundaries of the rectangular channel. Figure 1 depicts the flow geometry as well as the Cartesian coordinate system. At the start, both plates and fluid are not moving. After $t = 0^+$, these plates fluctuate having their velocities $\vec{V}_1(t) = u_1(0, t)\vec{e}_x$, $\vec{V}_2(t) = u_2(d, t)\vec{e}_x$, respectively. On that study



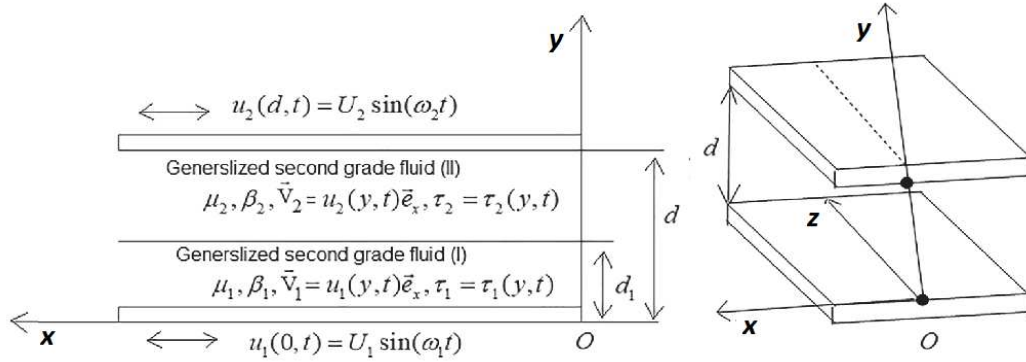


FIGURE 1. Flow geometry.

We will look at flow with velocity profiles

$$\vec{V}_i(y, t) = u_i(y, t)\vec{e}_x; \quad i = 1, 2. \quad (2.1)$$

The velocities indicated by Equation (2.1), of course, fulfil the equation of continuity $div(\vec{V}_i) = 0$. Suppose $D_1 = \{(x, y, z)/x \in \mathbf{R}, 0 \leq y \leq d_1, z \in \mathbf{R}\}$, $D_2 = \{(x, y, z)/x \in \mathbf{R}, d_1 \leq y \leq d, z \in \mathbf{R}\}$ be sub-regions of D_0 that is $D_0 = D_1 \cup D_2, d_1 < d$.

The flow's governing equations seem to be [22, 28, 30]:

In the region's $y \in [0, d_1]$ *second-grade fluid*:

$$\rho_1 \frac{\partial u_1}{\partial t} = \frac{\partial \tau_1}{\partial y}, \quad (2.2)$$

$$\tau_1 = \left(\mu_1 + \beta_1 \frac{\partial}{\partial t} \right) \frac{\partial u_1}{\partial y}. \quad (2.3)$$

In the region's $y \in [d_1, d]$ *second-grade fluid*:

$$\rho_2 \frac{\partial u_2}{\partial t} = \frac{\partial \tau_2}{\partial y}, \quad (2.4)$$

$$\tau_2 = \left(\mu_2 + \beta_2 \frac{\partial}{\partial t} \right) \frac{\partial u_2}{\partial y}, \quad (2.5)$$

where $\tau_i = S_{xy}^{(i)}(y, t)$; $i = 1, 2$ is the non-zero shear stress, μ_i denotes the viscosity of a fluid, a material coefficient is denoted by β_i , ρ_i denotes the fluid density.

We include all starting, boundary, and interfacial fluid-fluid characteristics in addition to the above equations

$$u_i(y, 0) = 0; \quad i = 1, 2, \quad y \in [0, d], \quad (2.6)$$

$$u_1(0, t) = U_1 \sin(\omega_1 t), \quad t \geq 0, \quad U_1 > 0, \quad (2.7)$$

$$u_2(d, t) = U_2 \sin(\omega_2 t), \quad t \geq 0, \quad U_2 > 0, \quad (2.8)$$

$$u_1(d_1, t) = u_2(d_1, t), \quad \tau_1(d_1, t) = \tau_2(d_1, t), \quad t \geq 0. \quad (2.9)$$

The following non-dimensional variables are introduced into Equations (2.2)-(2.9)

$$\begin{aligned} \tilde{x} &= \frac{x}{d}, \quad \tilde{y} = \frac{y}{d}, \quad \tilde{t} = \frac{t}{t_0}, \quad \tilde{u}_i = \frac{u_i}{U_1}, \quad \tilde{\tau}_i = \frac{\tau_i d}{\mu_1 U_1}, \quad \alpha_1 = \frac{\beta_1}{t_0 \mu_1}, \quad \gamma_1 = \frac{v_1 t_0}{d^2}, \quad a = \frac{\rho_2}{\rho_1}, \quad b = \frac{\mu_2}{\mu_1}, \quad h = \frac{d_1}{d}, \\ b &= \frac{\mu_2}{\mu_1}, \quad h = \frac{d_1}{d}, \quad \alpha_2 = \frac{\beta_2}{t_0 \mu_1}, \quad \tilde{\omega}_i = \omega_i t_0, \quad U_0 = \frac{U_2}{U_1}, \end{aligned} \quad (2.10)$$



where t_0 denotes the average time, and the non-dimensional governing equations are obtained (neglecting the " \sim " notation):

$$\frac{\partial u_1}{\partial t} = \gamma_1 \frac{\partial \tau_1}{\partial y}, \quad (2.11)$$

$$\tau_1 = \left(1 + \alpha_1 \frac{\partial}{\partial t}\right) \frac{\partial u_1}{\partial y}, \quad (2.12)$$

$$a \frac{\partial u_2}{\partial t} = \gamma_1 \frac{\partial \tau_2}{\partial y}, \quad (2.13)$$

$$\tau_2 = \left(b + \alpha_2 \frac{\partial}{\partial t}\right) \frac{\partial u_2}{\partial y}, \quad (2.14)$$

with the following initial and boundary conditions:

$$u_i(y, 0) = 0; \quad i = 1, 2, \quad y \in [0, 1], \quad (2.15)$$

$$u_1(0, t) = \sin(\omega_1 t), \quad t \geq 0, \quad (2.16)$$

$$u_2(1, t) = U_0 \sin(\omega_2 t), \quad t \geq 0, \quad (2.17)$$

$$u_1(h, t) = u_2(h, t), \quad \tau_1(h, t) = \tau_2(h, t), \quad t \geq 0. \quad (2.18)$$

The generalized fractional constitutive equations are now considered as follows:

$$\tau_1 = \left(1 + \alpha_1 D_t^{\delta_1}\right) \frac{\partial u_1}{\partial y}; \quad \delta_1 \in (0, 1], \quad (2.19)$$

$$\tau_2 = \left(b + \alpha_2 D_t^{\delta_2}\right) \frac{\partial u_2}{\partial y}; \quad \delta_2 \in (0, 1], \quad (2.20)$$

where $D_t^{\delta_i}$ where $i = 1, 2$, denotes the time fractional derivatives.

3. PRELIMINARIES

Now, we define the time-fractional Caputo, CF and ABC derivatives to used in fractional modeling of the above set of equations. These time derivatives are defined as:

3.1. Fractional derivative of Caputo: The fractional derivative of Caputo is stated as:

$${}^c D_t^{a_1} u(y, t) = \frac{1}{\Gamma(1 - a_1)} \int_0^t (t - s)^{-a_1} \frac{\partial u(y, s)}{\partial s} ds, \quad 0 < a_1 < 1, \quad (3.1)$$

its Laplace transform is [5, 14, 15]

$$\mathcal{L} \{ {}^c D_t^{a_1} u(y, t) \} = s^{a_1} \bar{u}(y, s) - u(y, 0). \quad (3.2)$$

3.2. Fractional derivative of Caputo-Fabrizio: The fractional derivative of Caputo-Fabrizio is stated as:

$${}^{CF} D_t^{b_1} u(y, t) = \frac{1}{1 - b_1} \int_0^t \exp\left(\frac{-b_1(t - s)}{1 - b_1}\right) \frac{\partial u(y, s)}{\partial s} ds, \quad 0 < b_1 < 1, \quad (3.3)$$

its Laplace transform is [9]

$$\mathcal{L} \{ {}^{CF} D_t^{b_1} u(y, t) \} = \frac{s \bar{u}(y, s) - u(y, 0)}{(1 - b_1)s + b_1}. \quad (3.4)$$



3.3. **Atangana-baleanu caputo(ABC) fractional derivative:** ABC fractional derivative stated as:

$${}^{ABC}D_t^{c_1}u(y, t) = \frac{1}{1 - c_1} \int_0^t E_{c_1} \left(\frac{-c_1(t - s)^{c_1}}{1 - c_1} \right) \frac{\partial u(y, s)}{\partial s} ds, \quad 0 \leq c_1 < 1, \tag{3.5}$$

where $E_{c_1}(-\tau^{c_1}) = \sum_{k=0}^{\infty} \frac{(-\tau)^{c_1 k}}{\Gamma(1+c_1 k)}$ is the generalized Mittag-leffler function. Its Laplace transform is [4]

$$\mathcal{L} \{ {}^{ABC}D_t^{c_1}u(y, t) \} = \frac{s^{c_1} \bar{u}(y, s) - u(y, 0)}{(1 - c_1)s^{c_1} + c_1}. \tag{3.6}$$

4. SOLUTION OF THE PROBLEM

4.1. **Solution of the problem via Caputo time fractional derivative:** By utilizing the Laplace transform and considering the initial conditions given in Equation (2.15), we can rewrite Equations (2.11), (2.13), (2.19), and (2.20) as follows:

$$s\bar{u}_1(y, s) = \gamma_1 \frac{\partial \bar{\tau}_1}{\partial y}, \tag{4.1}$$

$$as\bar{u}_2(y, s) = \gamma_2 \frac{\partial \bar{\tau}_2}{\partial y}, \tag{4.2}$$

$$\bar{\tau}_1(y, s) = (1 + \alpha_1 s^{a_1}) \frac{\partial \bar{u}_1}{\partial y}(y, s), \tag{4.3}$$

$$\bar{\tau}_2(y, s) = (b + \alpha_2 s^{a_2}) \frac{\partial \bar{u}_2}{\partial y}(y, s), \tag{4.4}$$

where the Laplace transform of the function $x(y, t)$ is represented by $\bar{x}(y, s) = \int_0^{\infty} x(y, t)e^{-st} dt$. The boundary and interface criteria must be satisfied by the Laplace transforms of $\bar{u}_i(y, s), i = 1, 2$.

$$\bar{u}_1(0, s) = \frac{\omega_1}{s^2 + \omega_1^2}, \quad \bar{u}_2(1, s) = \frac{U_0 \omega_2}{s^2 + \omega_2^2}, \tag{4.5}$$

$$\bar{u}_1(h, s) = \bar{u}_2(h, s), \quad \bar{\tau}_1(h, s) = \bar{\tau}_2(h, s). \tag{4.6}$$

Using Equations (4.3) and (4.4), into Equation (4.1) and (4.2), we get equations for velocity profiles with transform shapes:

$$s\bar{u}_1(y, s) = \gamma_1 (1 + \alpha_1 s^{a_1}) \frac{\partial^2 \bar{u}_1}{\partial y^2}(y, s), \tag{4.7}$$

$$as\bar{u}_2(y, s) = \gamma_2 (b + \alpha_2 s^{a_2}) \frac{\partial^2 \bar{u}_2}{\partial y^2}(y, s), \tag{4.8}$$

these have the following general solutions:

$$\bar{u}_1(y, s) = A_1(s)e^{-w_{11}(s)y} + B_1(s)e^{w_{11}(s)y}, \tag{4.9}$$

$$\bar{u}_2(y, s) = A_2(s)e^{-w_{12}(s)y} + B_2(s)e^{w_{12}(s)y}, \tag{4.10}$$

where

$$w_{11}(s) = \sqrt{\frac{s}{\gamma_1(1 + \alpha_1 s^{a_1})}}, w_{12}(s) = \sqrt{\frac{as}{\gamma_2(b + \alpha_2 s^{a_2})}}.$$

Using Equations (4.9) and (4.10) into Equations (4.3) and (4.4), we get equations for the shear stresses with transform shapes:

$$\bar{\tau}_1(y, s) = \frac{s}{\gamma_1 w_{11}(s)} [-A_1(s)e^{-w_{11}(s)y} + B_1(s)e^{w_{11}(s)y}], \tag{4.11}$$

$$\bar{\tau}_2(y, s) = \frac{s}{\gamma_2 w_{12}(s)} [-A_2(s)e^{-w_{12}(s)y} + B_2(s)e^{w_{12}(s)y}]. \tag{4.12}$$



The algebraic system imposes constraints on the new functions $A_i(s), B_i(s), i = 1, 2$.

$$\begin{aligned}\bar{u}_1(0, s) &= A_1(s) + B_1(s) = \frac{\omega_1}{s^2 + \omega_1^2}, \\ \bar{u}_2(1, s) &= A_2(s)e^{-w_{12}(s)} + B_2(s)e^{w_{12}(s)} = \frac{U_0\omega_2}{s^2 + \omega_2^2}, \\ \bar{u}_1(h, s) &= A_1(s)e^{-hw_{11}(s)} + B_1(s)e^{hw_{11}(s)} = A_2(s)e^{-hw_{12}(s)} + B_2(s)e^{hw_{12}(s)} = \bar{u}_2(h, s), \\ \bar{\tau}_1(h, s) &= \frac{s}{\gamma_1 w_{11}(s)} [-A_1(s)e^{-hw_{11}(s)} + B_1(s)e^{hw_{11}(s)}], \\ \bar{\tau}_2(h, s) &= \frac{s}{\gamma_1 w_{12}(s)} [-A_2(s)e^{-hw_{12}(s)} + B_2(s)e^{hw_{12}(s)}].\end{aligned}\tag{4.13}$$

The solutions of system (4.13) are:

$$\begin{aligned}A_1(s) &= \frac{D_1(s)}{D_0(s)}, \quad A_2(s) = \frac{D_2(s)}{D_0(s)}, \quad B_1(s) = \left(\frac{\omega_1}{s^2 + \omega_1^2} \right) - A_1(s), \\ B_2(s) &= \left(\frac{U_0\omega_2}{s^2 + \omega_2^2} \right) e^{-w_{12}(s)} - A_2(s)e^{-2w_{12}(s)},\end{aligned}$$

where

$$\begin{aligned}D_0(s) &= -2aw_{11}(s) \sinh(hw_{11}(s)) \left[e^{-(2-h)w_{12}(s)} + e^{-hw_{12}(s)} \right] + 2w_{12}(s) \cosh(hw_{11}(s)) \left[e^{-(2-h)w_{12}(s)} - e^{-hw_{12}(s)} \right], \\ D_1(s) &= aw_{11}(s) \left[e^{-(2-h)w_{12}(s)} + e^{-hw_{12}(s)} \right] F_1(s) - \left[e^{-(2-h)w_{12}(s)} - e^{-hw_{12}(s)} \right] F_2(s), \\ D_2(s) &= -2F_2(s) \sinh(hw_{11}(s)) + 2w_{12}(s) F_1(s) \cosh(hw_{11}(s)), \\ F_1(s) &= \left(-\frac{\omega_1}{s^2 + \omega_1^2} \right) e^{hw_{11}(s)} + \left(\frac{U_0\omega_2}{s^2 + \omega_2^2} \right) e^{-(1-h)w_{12}(s)}, \\ F_2(s) &= \left(-\frac{\omega_1}{s^2 + \omega_1^2} \right) w_{12}(s) e^{hw_{11}(s)} + a \left(\frac{U_0\omega_2}{s^2 + \omega_2^2} \right) w_{11}(s) e^{-(1-h)w_{12}(s)}.\end{aligned}$$

4.2. Solution of the problem via CF time fractional derivative: By utilizing the Laplace transform and considering the initial conditions given in Equation (2.15), we can rewrite Equations (2.19) and (2.20) as follows:

$$\bar{\tau}_1(y, s) = \left(1 + \frac{\alpha_1 s}{(1 - b_1)s + b_1} \right) \frac{\partial \bar{u}_1(y, s)}{\partial y},\tag{4.14}$$

$$\bar{\tau}_2(y, s) = \left(b + \frac{\alpha_2 s}{(1 - b_2)s + b_2} \right) \frac{\partial \bar{u}_2(y, s)}{\partial y}.\tag{4.15}$$

Using Equations (4.14) and (4.15) into Equations (4.1) and (4.2), we get equations for velocity profiles with transform shapes:

$$s\bar{u}_1(y, s) = \gamma_1 \left(1 + \frac{\alpha_1 s}{(1 - b_1)s + b_1} \right) \frac{\partial^2 \bar{u}_1(y, s)}{\partial y^2},\tag{4.16}$$

$$as\bar{u}_2(y, s) = \gamma_1 \left(b + \frac{\alpha_2 s}{(1 - b_2)s + b_2} \right) \frac{\partial^2 \bar{u}_2(y, s)}{\partial y^2},\tag{4.17}$$

these have the following general solutions:

$$\bar{u}_1(y, s) = C_1(s)e^{-w_{21}(s)y} + D_1(s)e^{w_{21}(s)y},\tag{4.18}$$

$$\bar{u}_2(y, s) = C_2(s)e^{-w_{22}(s)y} + D_2(s)e^{w_{22}(s)y},\tag{4.19}$$

where

$$w_{21}(s) = \sqrt{\frac{s[s(1 - b_1) + b_1]}{\gamma_1[(1 - b_1) + \alpha_1]s + b_1}}, \quad w_{22}(s) = \sqrt{\frac{as[s(1 - b_2) + b_2]}{\gamma_2[(b - bb_2 + \alpha_2)s + bb_2]}}.$$



Using Equations (4.18) and (4.19) into Equations (4.14) and (4.15), we get equations for the shear stresses with transform shapes:

$$\bar{\tau}_1(y, s) = \frac{s}{\gamma_1 w_{21}(s)} [-C_1(s)e^{-w_{21}(s)y} + D_1(s)e^{w_{21}(s)y}], \tag{4.20}$$

$$\bar{\tau}_2(y, s) = \frac{as}{\gamma_2 w_{22}(s)} [-C_2(s)e^{-w_{22}(s)y} + D_2(s)e^{w_{22}(s)y}]. \tag{4.21}$$

The algebraic system imposes constraints on the new functions $C_i(s), D_i(s), i = 1, 2$.

$$\begin{aligned} \bar{u}_1(0, s) &= C_1(s) + D_1(s) = \frac{\omega_1}{s^2 + \omega_1^2}, \\ \bar{u}_2(1, s) &= C_2(s)e^{-w_{22}(s)} + D_2(s)e^{w_{22}(s)} = \frac{U_0\omega_2}{s^2 + \omega_2^2}, \\ \bar{u}_1(h, s) &= C_1(s)e^{-hw_{21}(s)} + D_1(s)e^{hw_{21}(s)} = C_2(s)e^{-hw_{22}(s)} + D_2(s)e^{hw_{22}(s)} = \bar{u}_2(h, s), \\ \bar{\tau}_1(h, s) &= \frac{s}{\gamma_1 w_{21}(s)} [-C_1(s)e^{-hw_{21}(s)y} + D_1(s)e^{hw_{21}(s)y}], \\ \bar{\tau}_2(h, s) &= \frac{as}{\gamma_2 w_{22}(s)} [-C_2(s)e^{-hw_{22}(s)y} + D_2(s)e^{hw_{22}(s)y}]. \end{aligned} \tag{4.22}$$

The solutions of system (4.22) are:

$$\begin{aligned} C_1(s) &= \frac{D_{21}(s)}{D_{20}(s)}, \quad C_2(s) = \frac{D_{22}(s)}{D_{20}(s)}, \quad D_1(s) = \left(\frac{\omega_1}{s^2 + \omega_1^2} \right) - C_1(s), \\ D_2(s) &= \left(\frac{U_0\omega_2}{s^2 + \omega_2^2} \right) e^{-w_{22}(s)} - C_2(s)e^{-2w_{22}(s)}, \end{aligned}$$

where

$$\begin{aligned} D_{20}(s) &= -2aw_{21}(s) \sinh(hw_{21}(s)) \left[e^{-(2-h)w_{22}(s)} + e^{-hw_{22}(s)} \right] + 2w_{22}(s) \cosh(hw_{21}(s)) \left[e^{-(2-h)w_{22}(s)} - e^{-hw_{22}(s)} \right], \\ D_{21}(s) &= aw_{21}(s) \left[e^{-(2-h)w_{22}(s)} + e^{-hw_{22}(s)} \right] G_1(s) - \left[e^{-(2-h)w_{22}(s)} - e^{-hw_{22}(s)} \right] G_2(s), \\ D_{22}(s) &= -2G_2(s) \sinh(hw_{21}(s)) + 2w_{22}(s)G_1(s) \cosh(hw_{21}(s)), \\ G_1(s) &= \left(-\frac{\omega_1}{s^2 + \omega_1^2} \right) e^{hw_{21}(s)} + \left(\frac{U_0\omega_2}{s^2 + \omega_2^2} \right) e^{-(1-h)w_{22}(s)}, \\ G_2(s) &= \left(-\frac{\omega_1}{s^2 + \omega_1^2} \right) w_{22}(s)e^{hw_{21}(s)} + a \left(\frac{U_0\omega_2}{s^2 + \omega_2^2} \right) w_{21}(s)e^{-(1-h)w_{22}(s)}. \end{aligned}$$

4.3. Solution of the problem via ABC time fractional derivative: By utilizing the Laplace transform and considering the initial conditions given in Equation (2.15), we can rewrite Equations (2.19), and (2.20) as follows:

$$\bar{\tau}_1(y, s) = \left(1 + \frac{\alpha_1 s^{c_1}}{(1 - c_1)s^{c_1} + c_1} \right) \frac{\partial \bar{u}_1}{\partial y}(y, s), \tag{4.23}$$

$$\bar{\tau}_2(y, s) = \left(b + \frac{\alpha_2 s^{c_2}}{(1 - c_2)s^{c_2} + c_2} \right) \frac{\partial \bar{u}_2}{\partial y}(y, s). \tag{4.24}$$

Using Equations (4.23) and (4.24) into Equations (4.1) and (4.2), we get equations for velocity profiles with transform shapes:

$$s\bar{u}_1(y, s) = \gamma_1 \left(1 + \frac{\alpha_1 s^{c_1}}{(1 - c_1)s^{c_1} + c_1} \right) \frac{\partial^2 \bar{u}_1}{\partial y^2}(y, s), \tag{4.25}$$

$$as\bar{u}_2(y, s) = \gamma_1 \left(b + \frac{\alpha_2 s^{c_2}}{(1 - c_2)s^{c_2} + c_2} \right) \frac{\partial^2 \bar{u}_2}{\partial y^2}(y, s), \tag{4.26}$$



these have the following general solutions:

$$\bar{u}_1(y, s) = M_1(s)e^{-w_{31}(s)y} + N_1(s)e^{w_{31}(s)y}, \quad (4.27)$$

$$\bar{u}_2(y, s) = M_2(s)e^{-w_{32}(s)y} + N_2(s)e^{w_{32}(s)y}. \quad (4.28)$$

where

$$w_{31}(s) = \sqrt{\frac{s[(1-c_1)s^{c_1} + c_1]}{\gamma_1[(1-c_1 + \alpha_1)s^{c_1} + c_1]}}, \quad w_{32}(s) = \sqrt{\frac{as[(1-c_2)s^{c_2} + c_2]}{\gamma_2[(b-bc_2 + \alpha_2)s^{c_2} + bc_2]}}.$$

Using Equations (4.27) and (4.28) into Equations (4.23) and (4.24), we get equations for the shear stresses with transform shapes:

$$\bar{\tau}_1(y, s) = \frac{s}{\gamma_1 w_{31}(s)} [M_1(s)e^{-w_{31}(s)y} + N_1(s)e^{w_{31}(s)y}], \quad (4.29)$$

$$\bar{\tau}_2(y, s) = \frac{as}{\gamma_2 w_{32}(s)} [M_2(s)e^{-w_{32}(s)y} + N_2(s)e^{w_{32}(s)y}]. \quad (4.30)$$

The algebraic system imposes constraints on the new functions $M_i(s), N_i(s), i = 1, 2$.

$$\begin{aligned} \bar{u}_1(0, s) &= M_1(s) + N_1(s) = \frac{\omega_1}{s^2 + \omega_1^2}, \\ \bar{u}_2(1, s) &= M_2(s)e^{-w_{32}(s)} + N_2(s)e^{w_{32}(s)} = \frac{U_0\omega_2}{s^2 + \omega_2^2}, \\ \bar{u}_1(h, s) &= M_1(s)e^{-hw_{31}(s)} + N_1(s)e^{hw_{31}(s)} = M_2(s)e^{-hw_{32}(s)} + N_2(s)e^{hw_{32}(s)} = \bar{u}_2(h, s), \\ \bar{\tau}_1(h, s) &= \frac{s}{\gamma_1 w_{31}(s)} [-M_1(s)e^{-hw_{31}(s)} + N_1(s)e^{hw_{31}(s)}], \\ \bar{\tau}_2(h, s) &= \frac{as}{\gamma_2 w_{32}(s)} [-M_2(s)e^{-hw_{32}(s)} + N_2(s)e^{hw_{32}(s)}]. \end{aligned} \quad (4.31)$$

The solutions of system (4.31) are:

$$\begin{aligned} M_1(s) &= \frac{D_{31}(s)}{D_{30}(s)}, \quad M_2(s) = \frac{D_{32}(s)}{D_{30}(s)}, \quad N_1(s) = \left(\frac{\omega_1}{s^2 + \omega_1^2} \right) - M_1(s), \\ N_2(s) &= \left(\frac{U_0\omega_2}{s^2 + \omega_2^2} \right) e^{-w_{32}(s)} - M_2(s)e^{-2w_{32}(s)}, \end{aligned}$$

where

$$\begin{aligned} D_{30}(s) &= -2aw_{31}(s) \sinh(hw_{31}(s)) \left[e^{-(2-h)w_{32}(s)} + e^{-hw_{32}(s)} \right] + 2w_{32}(s) \cosh(hw_{31}(s)) \left[e^{-(2-h)w_{32}(s)} - e^{-hw_{32}(s)} \right], \\ D_{31}(s) &= aw_{31}(s) \left[e^{-(2-h)w_{32}(s)} + e^{-hw_{32}(s)} \right] K_1(s) - \left[e^{-(2-h)w_{32}(s)} - e^{-hw_{32}(s)} \right] K_2(s), \\ D_{32}(s) &= -2K_2(s) \sinh(hw_{31}(s)) + 2w_{32}(s)K_1(s) \cosh(hw_{31}(s)), \\ K_1(s) &= \left(-\frac{\omega_1}{s^2 + \omega_1^2} \right) e^{hw_{31}(s)} + \left(\frac{U_0\omega_2}{s^2 + \omega_2^2} \right) e^{-(1-h)w_{32}(s)}, \\ K_2(s) &= \left(-\frac{\omega_1}{s^2 + \omega_1^2} \right) w_{32}(s)e^{hw_{31}(s)} + a \left(\frac{U_0\omega_2}{s^2 + \omega_2^2} \right) w_{31}(s)e^{-(1-h)w_{32}(s)}. \end{aligned}$$

The analytical expressions for the Laplace transforms of $\bar{u}_1(y, s)$ and $\bar{u}_2(y, s)$ given by Equations (4.9), (4.10), (4.18), (4.19), (4.27), and (4.28) seem to be difficult, thus the inverse Laplace transforms $u_1(y, t)$, $u_2(y, t)$ would be derived



utilizing the numerical Stehfest's technique [1, 20, 31]. According to this technique, the velocities $u_i(y, t)$ are estimated by

$$u_i(y, t) \approx \frac{\ln(2)}{t} \sum_{k=1}^n S_k \bar{u}_i \left(y, \frac{k \ln(2)}{t} \right), t > 0, \tag{4.32}$$

where

$$S_k = (-1)^{k+\frac{n}{2}} \sum_{j=\lceil \frac{k+1}{2} \rceil}^{\min(k, \frac{n}{2})} \frac{j^{\frac{n}{2}} (2j)!}{\left(\frac{n}{2} - j\right)! j! (j-1)! (k-1)! (2j-k)!}, \tag{4.33}$$

where $[x]$ signifies the integer component of the real number x and n is an even natural number.

5. RESULTS AND DISCUSSION

This study examined the flow of two distinct, non-miscible, and incompressible generalized S.G fluids within a rectangular passageway. Fluid motion is created without the use of a pressure differential. A mathematical model based on constitutive equations of second-grade fluid with time-fractional C, CF and ABC time-fractional derivatives. Semi-analytical solutions to the problem, considering initial, boundary, and interface conditions, have been obtained by utilizing the Laplace transform in conjunction with Stehfest's technique for performing numerical inverse Laplace transforms. Utilizing Mathcad software, numerical results have been derived and visually represented for the shear stress and fluid velocity. Various aspects of fluid motion are illustrated in Figures 2, 3, 4, 5, and 6, which are drawn for distinct fractional parameters $a_1, a_2, b_1, b_2, c_1,$ and c_2 in $C, CF,$ and $ABC,$ respectively. (additional parameters are specified in the labels of the figures).

By employing the defining equation, we can underscore the impact of the C fractional derivative (F.D) on the strain-rate tensor elements. Alternatively, Equations (4.3) can be written in the following form.

$$\frac{\partial \bar{u}(y, s)}{\partial y} = \frac{1}{1 + \alpha_1 s^{\alpha_1}} \bar{\tau}(y, s), \tag{5.1}$$

Therefore, the velocity gradient is given by a convolution.

$$\frac{\partial u(y, t)}{\partial y} = \phi(a_1, t) * \tau_1(y, t) = \int_0^t \phi(a_1, t-r) * \tau_1(y, r) dr, \tag{5.2}$$

where, the kernel $\phi(a_1, t)$:

$$\phi(a_1, t) = \frac{1}{\alpha_1} t^{\alpha_1-1} E_{\alpha_1, \alpha_1} \left(\frac{-t^{\alpha_1}}{\alpha_1} \right), \tag{5.3}$$

where $E_{a,b}(\cdot)$ is the Mittag-Leffler function of two-parameters.

By employing the defining equation, we can underscore the impact of the CF F.D on the strain-rate tensor elements. Alternatively, Equation (4.14) can be written in the following form.

$$\frac{\partial \bar{u}(y, s)}{\partial y} = \frac{s(1 - b_1) + b_1}{(1 - b_1 + \alpha_1)s + b_1} \bar{\tau}(y, s), \tag{5.4}$$

Therefore, the velocity gradient is given by a convolution.

$$\frac{\partial u(y, t)}{\partial y} = \phi(b_1, t) * \tau_1(y, t) = \int_0^t \phi(b_1, t-r) * \tau_1(y, r) dr, \tag{5.5}$$

where, the kernel $\phi(b_1, t)$:

$$\phi(b_1, t) = \frac{1 - b_1}{1 - b_1 + \alpha_1} \left\{ \delta(t) - \frac{b_1}{1 - b_1 + \alpha_1} e^{\frac{-b_1 t}{1 - b_1 + \alpha_1}} \right\} + \frac{b_1}{1 - b_1 + \alpha_1} e^{\frac{-b_1 t}{1 - b_1 + \alpha_1}}, \tag{5.6}$$

where $\delta(t)$ is a dirac delta function.



By employing the defining equation, we can underscore the impact of the *ABC* F.D on the strain-rate tensor elements. Alternatively, Equation (4.23) can be written in the following form.

$$\frac{\partial \bar{u}(y, s)}{\partial y} = \frac{s^{c_1}(1 - c_1) + c_1}{(1 - c_1 + \alpha_1)s^{c_1} + c_1} \bar{\tau}(y, s), \quad (5.7)$$

Therefore, the velocity gradient is given by a convolution.

$$\frac{\partial u(y, t)}{\partial y} = \phi(c_1, t) * \tau_1(y, t) = \int_0^t \phi(c_1, t - r) * \tau_1(y, r) dr, \quad (5.8)$$

where, the *kernel* $\phi(c_1, t)$:

$$\phi(c_1, t) = \frac{1 - c_1}{1 - c_1 + \alpha_1} \left\{ \delta(t) - \frac{c_1 t^{c_1 - 1}}{1 - c_1 + \alpha_1} E_{c_1, c_1} \left(\frac{-c_1 t^{c_1}}{1 - c_1 + \alpha_1} \right) \right\} + \frac{c_1 t^{c_1 - 1}}{1 - c_1 + \alpha_1} E_{c_1, c_1} \left(\frac{-c_1 t^{c_1}}{1 - c_1 + \alpha_1} \right), \quad (5.9)$$

where $E_{a,b}(\cdot)$ is the *Mittag-Leffler* function of two-parameters and $\delta(t)$ is a dirac delta function.

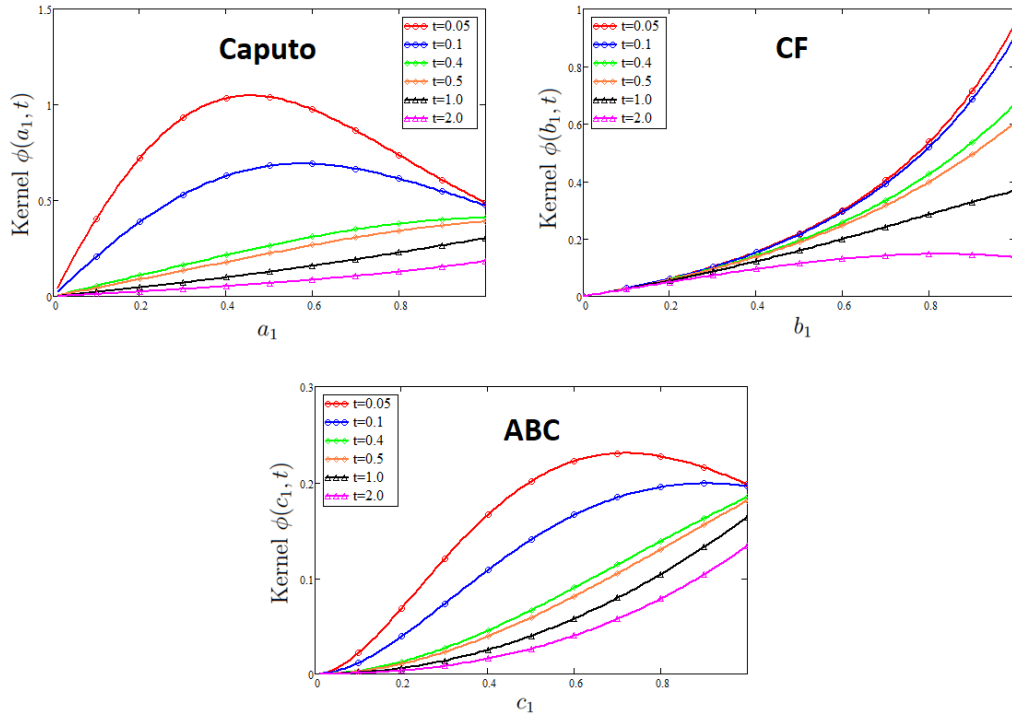


FIGURE 2. The profile of the *damping kernel* (D.K) $\phi(a_1, t)$, $\phi(b_1, t)$, and $\phi(c_1, t)$ for different values of t of **Caputo**, **CF**, and **ABC**, respectively.

The shear stress history, as indicated by Equations (5.2), (5.5), and (5.8), has a significant impact on the velocity gradient and, consequently, on fluid motion. Figure 2 illustrates the variations of the *damping kernel* (D.K) $\phi(a_1, t)$, $\phi(b_1, t)$, and $\phi(c_1, t)$ for $t \in \{0.05, 0.1, 0.4, 0.5, 1.0, 2.0\}$ and for memory parameters $a_1, b_1, c_1 \in [0, 1]$.

The analysis of Figure 2 indicates that the D.K is essential for small t and for the fractional parameters a_1, b_1, c_1 in *C*, *CF*, and *ABC*, respectively. In contrast, for larger t values, the D.K demonstrates a nearly linear relationship with the fractional parameters, with its values decreasing as t advances. Thus, the impact of the fractional derivative becomes less significant as time progresses. This trend is clearly illustrated in the *Figures* depicting the velocity and

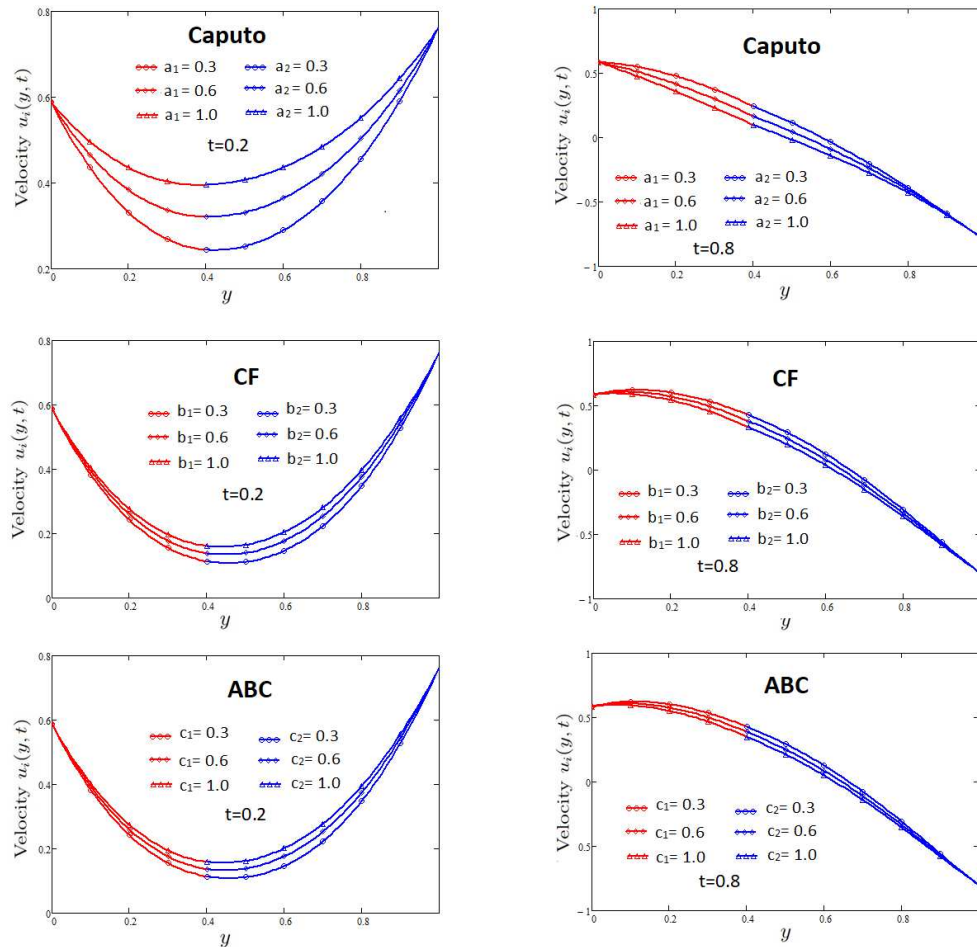


FIGURE 3. For $t = 0.2, 0.4$ and various fractional parameters values a_1, a_2, b_1, b_2, c_1 and c_2 , the velocity profiles $u_i(y, t)$ where $i = 1, 2$ of **Caputo**, **CF** and **ABC**.

shear stress profiles, specifically in Figures 2-6. Following parameter values were used in Figures: $h = 0.4, U_0 = 0.8, \omega_1 = \pi, \omega_2 = 2\pi, \alpha_1 = 0.5, \alpha_2 = 0.8, \gamma_1 = 0.3, a = 0.6, b = 0.8$.

Figures 3 and 4 show the effect of a_1, a_2, b_1, b_2, c_1 , and c_2 on the profiles of velocity and shear stress of C, CF and ABC for $t = 0.2$ and $t = 0.4$. The first layer of the second-grade fluid, defined by a velocity of $u_1(y, t)$ and a shear stress of $\tau_1(y, t)$, exists within the range of $y \in [0, 0.4]$. In contrast, the second layer of the *second*-grade fluid, which has a velocity of $u_2(y, t)$ and a shear stress of $\tau_2(y, t)$, is found in the region where $y \in [0.4, 1]$.

The analysis presented in Figures 3-6 reveals that memory effects are notably crucial for small time t and fractional parameters. Under these conditions, fluids governed by fractional constitutive equations exhibit slower flow rates compared to ordinary fluids. This observation is consistent with the behavior of the D.K, as illustrated in Figure 2.

For these specific time and fractional parameter values, the velocity gradient is more significantly damped, resulting in lower velocity magnitudes. In the examined scenario, ordinary fluids exhibit slower flow rates compared to fractional fluids at $t \geq 0.4$ in C , and at $t \geq 0.8$ in CF and ABC , attributed to the time-dependent reduction of the damping kernel.

Figure 5 illustrates the shear stress and fluid velocity at the liquid-liquid interface, incorporating C, CF , and ABC time-fractional derivatives, for various values of the fractional parameters a_1, a_2, b_1, b_2, c_1 , and c_2 when $y = h$. Figure



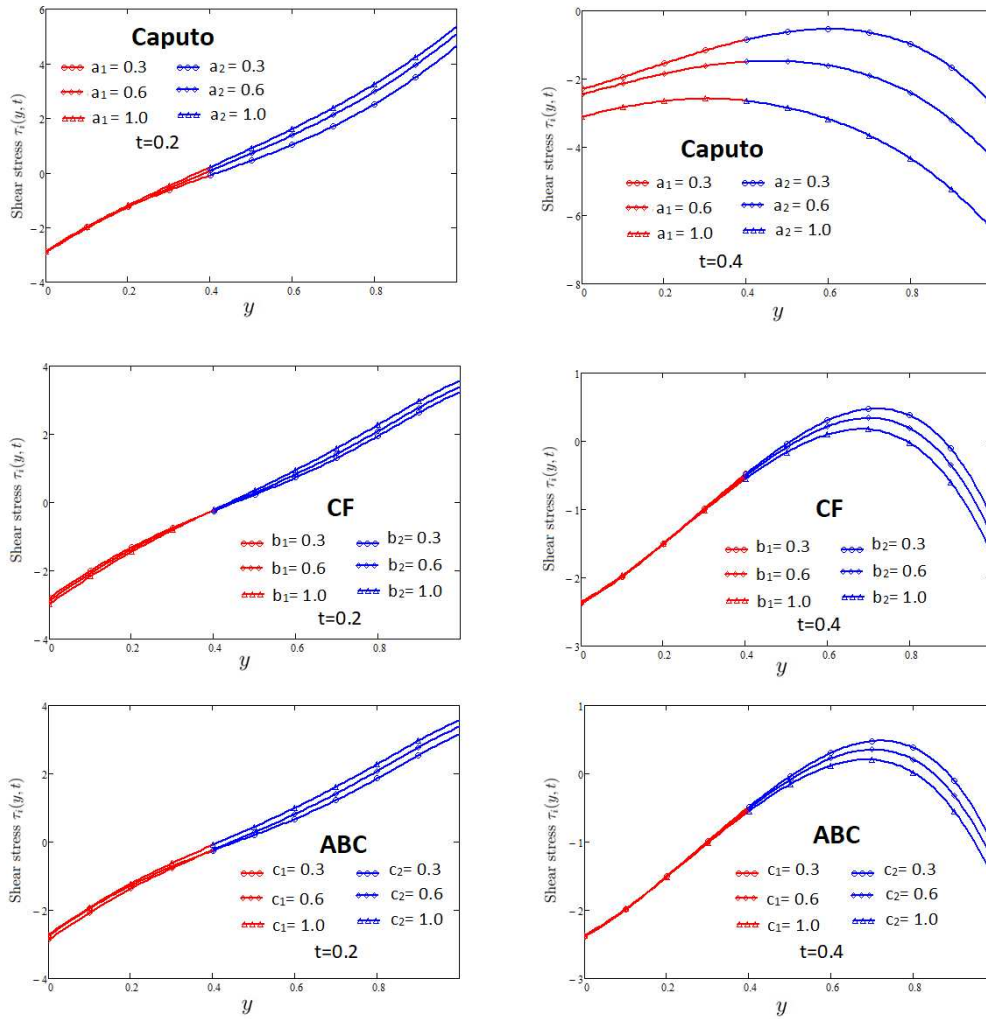


FIGURE 4. For $t = 0.2, 0.4$ and various fractional parameters values a_1, a_2, b_1, b_2, c_1 and c_2 , the shear stress profiles $\tau_i(y, y)$ where $i = 1, 2$ of **Caputo**, **CF** and **ABC**.

6 depicts the shear stress and fluid velocity at the channel boundaries located at $y = 0$ and $y = 1$, corresponding to various values of the fractional parameters a_1, a_2, b_1, b_2, c_1 , and c_2 . The concavity in Figures 5 and 6 can be seen. On the interface, the behavior of velocity and shear stress is similar in C, CF and ABC . The memory effects are substantially larger for low values of time t , as seen in Figures 5 and 6. The damping values are negligible for high values of time t , hence the fractional parameter has very little effect on the fluid behavior. Further we have drawn a comparison between the C, CF and ABC fractional S.G fluids in Figure 7 and their corresponding values are shown in Tables 1 and 2. Observations indicate that there is a significant alignment among these fractional fluids.

6. CONCLUSIONS

In this study we have investigated the unsteady one-dimensional flows of two generalized S.G fluids that are immiscible and incompressible in a rectangle. The channel walls have fluctuating translational motions in the plane, while acting in the flow direction. Multiple mathematical frameworks constructed upon generalized fractional governing



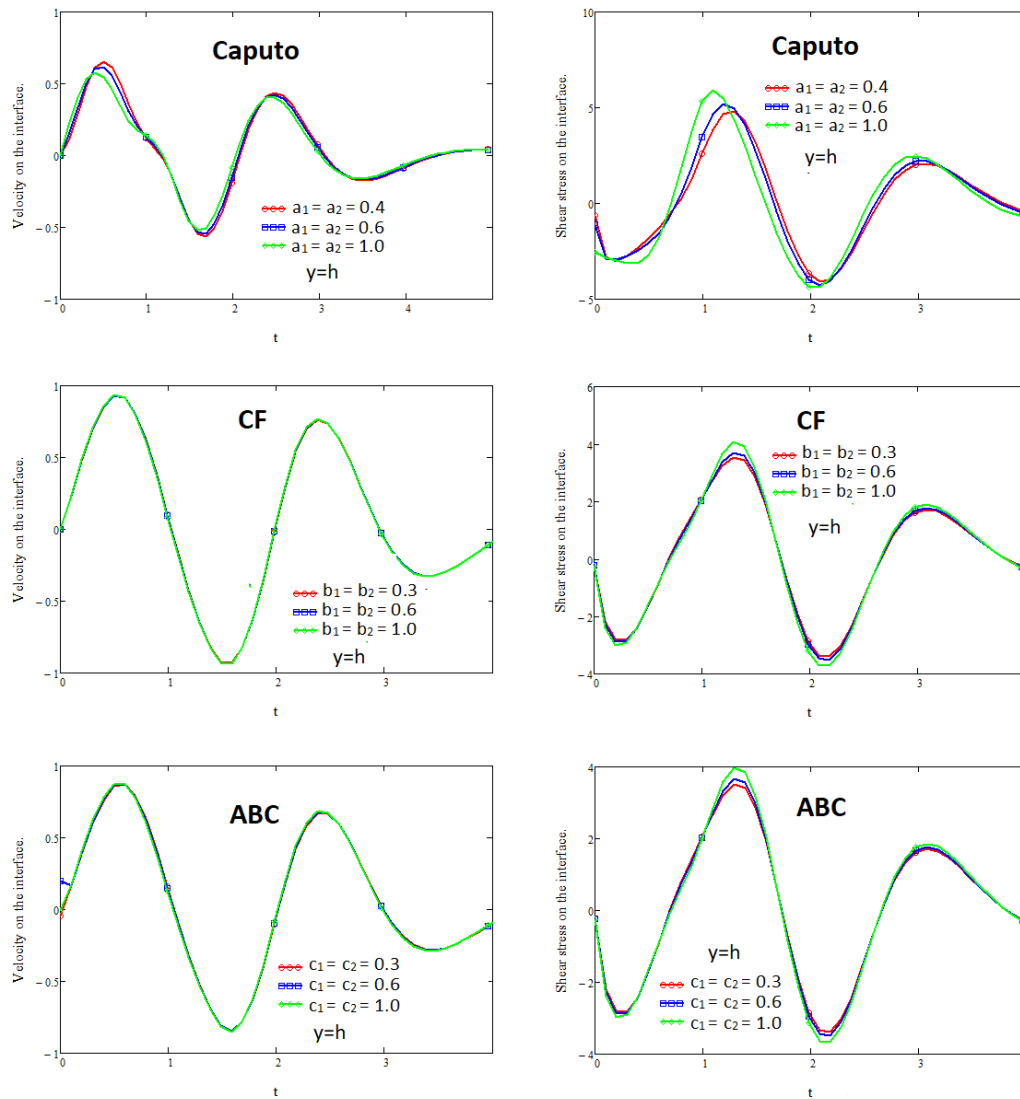


FIGURE 5. The shear stress and velocity diagrams for the constitutive equation of a S.G fluid involving **Caputo**, **CF**, and **ABC** time-fractional derivatives at the liquid-liquid interface.

equations having time-fractional derivatives C , CF and ABC . In such mathematical frameworks, the evolution of a shear stress has an impact on the velocity gradient. Utilizing the Laplace transform, semi-analytical solutions for the fluid velocity and shear stress have been found. The Stehfest numerical algorithm was used to obtain the inverse Laplace transforms. Through numerical simulations, the effect of the fractional parameters on the velocity and shear stress has been investigated graphically using the software Mathcad. Memory effects are seen to be important only for small time t .

Data Availability Statement. All the data used is presented in the paper.

Funding. Not applicable.



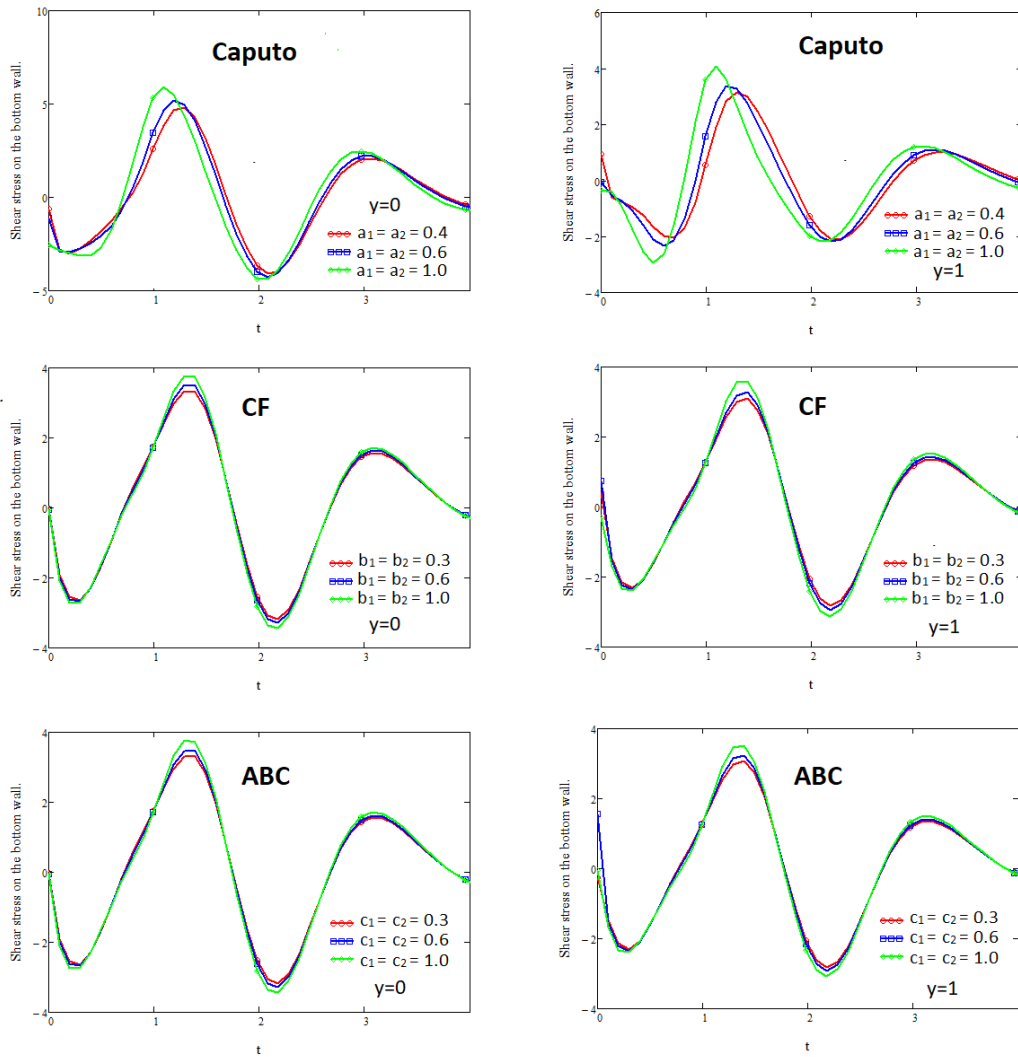


FIGURE 6. The shear stress upon that channel walls for various fractional parameters a_1 , a_2 , b_1 , b_2 , c_1 , and c_2 are shown in the diagrams.

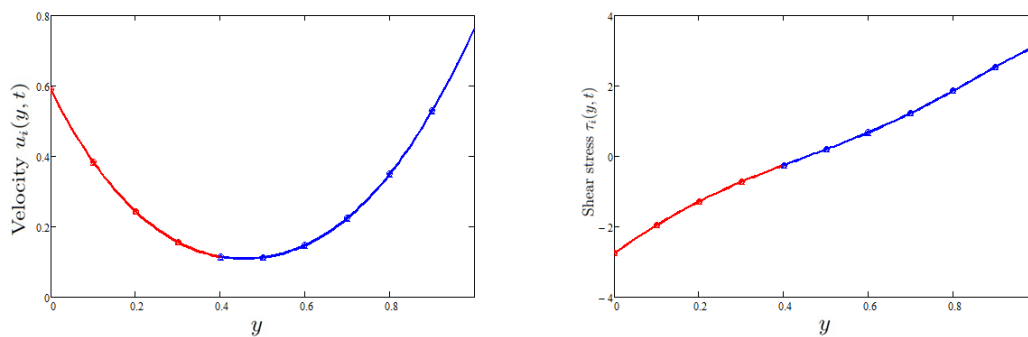


FIGURE 7. Comparison between the Caputo, CF and ABC fractional time derivatives for time $t = 0.2$.

TABLE 1. Comparison of velocity components $u_1(y, t)$ and $u_2(y, t)$ using different fractional derivatives.

y	Velocity $u_1(y, t)$			Velocity $u_2(y, t)$		
	Caputo	CF	ABC	Caputo	CF	ABC
0.1	0.385	0.383	0.383	0.369	0.363	0.362
0.2	0.245	0.243	0.243	0.236	0.234	0.233
0.3	0.158	0.156	0.156	0.155	0.153	0.153
0.4	0.115	0.114	0.113	0.115	0.114	0.114
0.5	0.113	0.112	0.111	0.113	0.112	0.112
0.6	0.151	0.150	0.148	0.149	0.147	0.147
0.7	0.233	0.234	0.227	0.226	0.224	0.224
0.8	0.363	0.372	0.351	0.351	0.349	0.348
0.9	0.541	0.572	0.514	0.530	0.528	0.528
1.0	0.734	0.753	0.723	0.762	0.761	0.761

TABLE 2. Comparison of shear stress $\tau_1(y, t)$ and $\tau_2(y, t)$ using different fractional derivatives.

y	Shear stress $\tau_1(y, t)$			Shear stress $\tau_2(y, t)$		
	Caputo	CF	ABC	Caputo	CF	ABC
0.1	-1.958	-1.953	-1.951	-2.006	-1.938	-1.920
0.2	-1.286	-1.281	-1.280	-1.298	-1.276	-1.269
0.3	-0.728	-0.725	-0.725	-0.733	-0.725	-0.722
0.4	-0.251	-0.248	-0.251	-0.252	-0.250	-0.249
0.5	0.199	0.202	0.192	0.201	0.202	0.199
0.6	0.675	0.687	0.656	0.682	0.679	0.677
0.7	1.211	1.252	1.165	1.232	1.229	1.226
0.8	1.782	1.921	1.670	1.865	1.863	1.859
0.9	2.223	2.678	1.964	2.541	2.544	2.539
1.0	2.793	3.486	2.706	3.147	3.157	3.152



REFERENCES

- [1] J. Abate and W. Whitt, *A unified framework for numerically inverting Laplace transforms*, *INFORMS Journal on Computing*, 18(4) (2006), 408-421.
- [2] K. A. Abro, *Porous effects on second grade fluid in oscillating plate*, *Journal Applied Environmental Biological Science*, 6(5) (2016), 17-82.
- [3] A. Ali Zafar, M. Bilal Riaz, and M. Imran Asjad, *Unsteady rotational flow of fractional Maxwell fluid in a cylinder subject to shear stress on the boundary*, *Punjab University Journal of Mathematics*, 50(2) (2020).
- [4] A. Atangana and D. Baleanu, *New fractional derivatives with non-local and nonsingular kernel. Theory and application to Heat transfer model*, arXiv preprint arXiv:1602.03408, 20 (2016), 763-769.
- [5] D. Baleanu, K. Diethelm, and E. Scalas, *Fractional Calculus: Models and Numerical Methods*, World Scientific, 3 2012.
- [6] D. Baleanu and J. Hristov, *Fractional dynamics in natural phenomena and advanced technologies*, Cambridge Scholars Publishing, (Eds.), (2024).
- [7] D. Baleanu, A. Mousalou, and S. Rezapour, *The extended fractional Caputo-Fabrizio derivative of order $0 \leq \sigma < 1$ on $CR [0, 1]$ and the existence of solutions for two higher-order series-type differential equations*, *Advances in Differential Equations*, Springer, 2018(1) (2018), 1-11.
- [8] S. Bilal, A. H. Majeed, R. Mahmood, I. Khan, A. H. Seikh, and E. S. M. Sherif, *Heat and mass transfer in hydromagnetic second-grade fluid past a porous inclined cylinder under the effects of thermal dissipation, diffusion and radiative heat flux*, *Energies*, 13(1) (2020), 278.
- [9] M. Caputo and M. Fabrizio, *A new definition of Fractional differential without singular kernel*, *Prog. Fract. Differ. Appl.*, 1(2) (2015), 73-85.
- [10] C. O. K. Chen, H. Y. Lai, and W. F. Chen, *Unsteady unidirectional flow of second-grade fluid through a microtube with wall slip and different given volume flow rate*, *Mathematical problems in Engineering*, 2010(1) (2010), 416837.
- [11] M. E. Erdogan and C. E. Imrak, *Steady flow of a second-grade fluid in an annulus with porous walls*, *Mathematical Problems in Engineering*, 2008(1) (2008), 867906.
- [12] M. Faryad, S. Farid, S. Riaz, and I. Bhatti, *Fully developed liquid layer flow over a convex corner considering surface tension effects using numerical methods*, *Punjab University Journal of Mathematics*, 47(2) (2020).
- [13] A. I. Fedorchenko, *Introduction to fractional calculus*, Czech Republic, (2008).
- [14] R. Hilfer, *Mathematical and Physical interpretations of fractional derivatives and integrals*, *Handbook of Fractional Calculus with Application*, 1 (2019), 47-85.
- [15] J. Hristov, *Response functions in linear viscoelastic constitutive equations and related functional operators*, *Mathematical modeling of Natural Phenomena*, 14(3) (2019), 305.
- [16] M. Javaid, M. Imran, M. A. Imran, I. Khan and K. S. Nisar, *Natural convection flow of a second grade fluid in an infinite vertical cylinder*, *Scientific Reports*, 10(1) (2020), 8327.
- [17] M. Khan and M. U. Rahman, *Flow and heat transfer to modified second grade fluid over a non-linear stretching sheet* *AIP Advances*, 5(8) (2015).
- [18] M. Khan, S. Nadeem, T. Hayat, and A. M. Siddiqui, *Unsteady motions of a generalized second-grade fluid*, *Mathematical and Computer Modelling*, 41(6-7) (2005), 629-637.
- [19] A. A. Kilbas, *Theory and applications of fractional differential equations* North-Holland Mathematics Studie, 204 (2006).
- [20] K. L. Kuhlman, *Review of inverse Laplace transform algorithms for Laplace-space numerical approaches*, *Numerical Algorithms*, 63(2) (2013), 339-355.
- [21] M. P. Lazarevic, M. R. Rapaic, T. B. Ekara, V. Mladenov, and N. Mastorakis, *Introduction to fractional calculus with brief historical background*, *Advanced Topics on Applications of Fractional Calculus on Control Problems, System Stability and Modeling*, (2014), 3-16.
- [22] H. Luo, M. G. Blyth, and C. Pozrikidis, *Two-layer flow in a corrugated channel*, *Journal of Engineering Mathematics*, 60(2) (2008), 127-147.
- [23] L. Luo, N. A. Shah, I. M. Alarifi, and D. Vieru, *Two-layer flows of generalized immiscible second grade fluids in a rectangular channel*, *Mathematical Methods in the Applied Sciences*, 43(3) (2020), 1337-1348.



- [24] A. Mahmood, C. Fetecau, N. A. Khan, and M. Jamil, *Some exact solutions of the oscillatory motion of a generalized second grade fluid in an annular region of two cylinders*, Acta Mechanica Sinica, 26(4) (2010), 541-550.
- [25] M. Naeem, H. Rezazadeh, A. A. Khammash, R. Shah, and S. Zaland *Analysis of the Fuzzy Fractional-Order Solitary Wave Solutions for the KdV Equation in the Sense of Caputo-Fabrizio Derivative*, Journal of Mathematics, 2022(1) (2022), 3688916.
- [26] Y. Povstenko and T. Kyrylych, *Time-fractional heat conduction in a plane with two external half-infinite line slits under heat flux loading*, Symmetry, 11(5) (2019), 689.
- [27] Y. Z. Povstenko, *Fractional Cattaneo-type equations and generalized thermoelasticity*, Journal of thermal Stresses, 34(2) (2011), 97-114.
- [28] A. M. Siddiqui, T. Haroon, Z. Bano, and J. H. Smeltzer, *Steady 2-D flow of a second grade fluid in a symmetrical diverging channel of varying width*, Applied Mathematical Sciences, 8(94) (2014), 4675-4691.
- [29] A. M. Siddiqui, A. Walait, T. Allison, and T. Haroon, *Exact solution for pressure driven flow of two immiscible Phan-Thien-Tanner fluids in a pipe*, Open Journal of Fluid Dynamics, 8(04) (2018), 378.
- [30] A. M. Siddiqui, M. Zeb, T. Haroon, and Q. U. A. Azim, *Exact solution for the heat transfer of two immiscible PTT fluids flowing in concentric layers through a pipe*, Mathematics, 7(1) (2019), 81.
- [31] H. Stehfest, *Algorithm 368: Numerical inversion of Laplace transforms [D5]*, Communications of the Association for Computing Machinery, 13(1) (1970), 47-49.
- [32] Z. U. A. Zafar, N. Sene, H. Rezazadeh, and N. Esfandian, *Tangent nonlinear equation in context of fractal fractional operators with nonsingular kernel*, Mathematical Sciences, 16(2) (2022), 121-131.
- [33] Z. Zheng, W. Zhao, and H. Dai, *A new definition of fractional derivative*, International Journal of Non-Linear Mechanics, 108 (2019), 1-6.
- [34] M. X. Zhou, A. S. V. R. Kanth, K. Aruna, K. Raghavendar, H. Rezazadeh, M. Inc, and A. A. Aly, *Numerical Solutions of Time Fractional Zakharov-Kuznetsov Equation via Natural Transform Decomposition Method with Nonsingular Kernel Derivatives*, Journal of Function Spaces, 2021 (2021).

Uncorrected Proof

